

Explaining the Hemispheric Pattern of Filament Chirality

Duncan H. Mackay¹ and Anthony R. Yeates²

¹School of Mathematics and Statistics, University of St Andrews, St Andrews, KY16 8HB, UK
email: duncan@mcs.st-and.ac.uk

²Department of Mathematical Sciences, Durham University, Durham, UK
email: anthony.yeates@durham.ac.uk

Abstract. Solar filaments are known to exhibit a hemispheric pattern in their chirality, where dextral/sinistral filaments dominate in the northern/southern hemisphere. We show that this pattern may be explained through data driven 3D global magnetic field simulations of the Sun's large-scale magnetic field. Through a detailed comparison with 109 filaments over a 6 month period, the model correctly reproduces the filament chirality and helicity with a 96% agreement. The data driven simulation is extended to run over a full solar cycle, where predictions are made for the spatial and temporal dependence of the hemispheric pattern over the solar cycle.

Keywords. Sun: filaments, Sun: magnetic fields, Sun: prominences

1. Introduction

In recent years, solar filaments have been classified by the orientation of their main axial magnetic field. This orientation, named the filament chirality (Martin *et al.*, 1994) may take one of two forms: dextral or sinistral. Dextral/sinistral filaments have an axial magnetic field that points to the right/left when the main axis of the filament is viewed from the positive polarity side of the PIL. A dextral filament is expected to contain dominantly negative helicity, a sinistral filament positive helicity. As filaments and their channels form over a wide range of latitudes on the Sun, they may be regarded as useful indicators of sheared non-potential fields and magnetic helicity.

A surprising feature of the chirality of filaments is that it displays a large-scale hemispheric pattern: dextral/sinistral filaments dominate in the northern/southern hemispheres, respectively (Martin *et al.*, 1994; Zirker *et al.*, 1997; Yeates *et al.*, 2007). Although dextral/sinistral filaments dominate in the northern/southern hemisphere, observations show that exceptions to this pattern do occur. Any model which tries to explain the formation of filaments must explain not only the origin of this hemispheric pattern but also why exceptions to it arise.

2. Global Non-linear Force-Free Field Model

To explain the hemispheric pattern of solar filaments we will apply a global non-linear force-free magnetic field model. The model developed by van Ballegooijen *et al.* (2000) and Mackay & van Ballegooijen (2006) considers the long-term evolution of coronal magnetic fields. The technique describes the build-up of free magnetic energy and electric currents in the corona by coupling together two distinct models. The first is a data driven surface flux transport model (Yeates *et al.*, 2007). This models the large-scale surface motions of differential rotation, meridional flow and surface diffusion. In addition

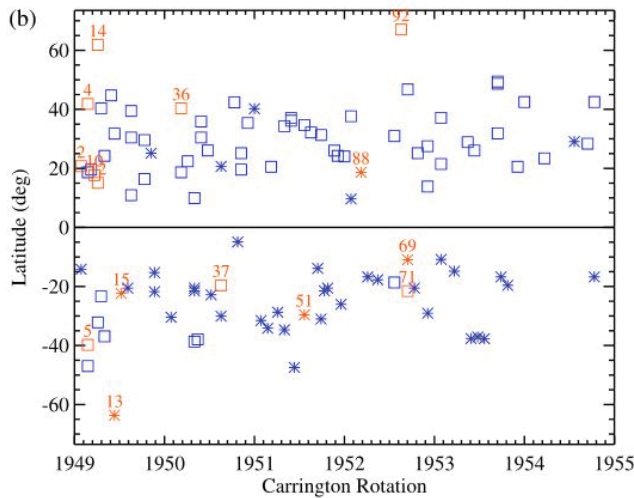


Figure 1. Results of the comparison between theory and observations. The symbols denote the observed chirality of each filament (squares \sim dextral, stars \sim sinistral). The color denotes agreement between the simulation and observations (blue \sim correct chirality in simulation, red \sim incorrect chirality in simulation). A color version is available online.

to this observations of newly emerging magnetic bipoles are included to produce a continuous evolution of the observed photospheric magnetic flux over long periods of time. Coupled to this is a quasi-static coronal evolution model (Mackay & van Ballegoijen, 2006; Yeates *et al.*, 2008) which evolves the coronal magnetic field through a sequence of nonlinear force-free fields in response to the observed photospheric evolution and flux emergence.

3. Six Month Comparison Between Theory and Observations

To determine the origin of the hemispheric pattern of filaments we carry out a direct comparison between theory and observations (see Yeates *et al.*, 2007; Yeates *et al.*, 2008). First, $H\alpha$ observations from BBSO over a 6 month period are studied to determine the location and chirality of 109 filaments (Yeates *et al.*, 2007) relative to the underlying magnetic flux. In Figure 1 the symbols denote the observed chirality of each filament (squares \sim dextral, stars \sim sinistral). It is clear that the dominant chirality pattern occurs in each hemisphere, but also a number of exceptions exist. Next the combined magnetic flux transport and magneto-frictional simulations (Section 2), based on actual photospheric magnetic distributions found on the Sun is run. The run is carried out for the whole six month period without ever resetting the surface field back to that found in observations or the coronal field to potential. To maintain accuracy over this time, 119 bipoles are emerged within the simulations where their properties (location, size, flux, tilt angle) are determined from observations. The simulations describe the long term helicity transport across the solar surface from low to high latitudes.

A direct one-to-one comparison of the chirality produced by the model and the observed chirality of the filaments is carried out (Yeates *et al.*, 2008). Through varying the sign and amount of helicity emerging within the bipoles and by emerging dominantly negative helicity in the northern hemisphere and positive in the southern, a 96% agreement can be found between the observations and simulations. The locations where the simulations

produce the same chirality as the observations are shown in blue. Where they disagree and the simulations produce the incorrect chirality are shown in red. An important feature is that the agreement is equally good for minority chirality filaments as well as for dominant chirality filaments. A key feature of the simulations is that a better agreement between the observations and simulations is found the longer the simulations are run. The majority of the disagreements arise within the first six months. This indicates that the Sun has a long term memory of the transport of helicity from low to high latitudes. The reason for this high agreement is described in the paper of Yeates & Mackay (2009).

The results demonstrate that the combined effects of differential rotation, meridional flow, supergranular diffusion along with the emergence of non-potential active regions are sufficient to produce the observed hemispheric pattern of filaments. While the model obtained an excellent agreement with the observed chirality of filaments, the 6 month simulation was unable to reproduce dextral/sinistral chirality along the polar crown PILs in the northern/southern hemispheres. Note that filament 92 that lies at 68° latitude between CR1952 and CR1953 is incorrect. This is due to the fact that the simulation was not run for long enough to transport helicity from low to high latitudes which occurs over the meridional flow timescale of 2 year. The topic of the polar crown chirality will be considered in the next section.

4. Full Solar Cycle Predictions

To consider the chirality at high latitudes a longer simulation is run for a full solar cycle (Yeates & Mackay, 2012). The simulation is initialised with a potential field extrapolation based on a Kitt Peak synoptic magnetogram for Carrington Rotation CR1910, corrected for differential rotation to represent 1996 May 15. The coronal magnetic field is then continuously evolved. Over the 15 year period 1838 active regions are emerged where their flux varies from 2×10^{20} Mx to 5.3×10^{22} Mx.

Figure 2(a) shows a longitudinal average of the photospheric radial magnetic field B_{0r} in the simulation which reproduces well the observed field. Figure 2(b) shows the longitude-averaged skew angle along PILs where red denotes dextral skew and blue sinistral skew. Several features are apparent: (a) Below $\pm 50^\circ$ latitude the majority pattern of chirality predominates, i.e., dextral in the northern hemisphere and sinistral in the southern hemisphere, although the overall pattern has significant fluctuations (minority chirality exists at all latitudes in each hemisphere); (b) During the period of few active regions from 2007 to 2010, there is a more mixed chirality at lower latitudes; (c) Until 1998 and during the declining phase from 2001 to 2006, there is a tendency for minority chirality on the high-latitude PILs (sinistral in the north, dextral in the south); (d) During the rush-to-the-poles between 1998 and mid-1999, the polar crowns exhibit the majority chirality pattern; (e) From 2006 onward, the majority chirality dominates at high latitudes once more, continuing into Cycle 24.

It should be noted that the minority chirality at high-latitudes in either hemisphere until 1998 is due the initial condition which is a potential field. Once this is removed by the transport of helicity poleward which occurs over a 2 year time period the correct chirality is found at high latitudes in the rising phase. Note that due to the continuous nature of the simulation, from 2006 onwards the correct chirality is found at high latitudes in the rising phase of the present cycle. This indicates that the incorrect results for filament 92, which lies at high latitudes (Figure 1), was a result of the simulation not being run for long enough.

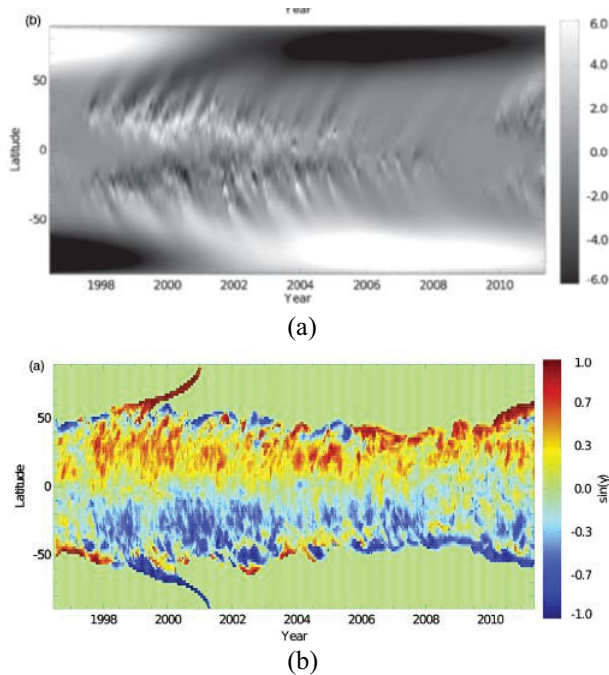


Figure 2. Butterfly diagrams showing longitude-averaged over Cycle 23. (a) Radial magnetic field B_{0r} in the simulation and (b) skew $\sin \gamma$ measured at height $r = 1.033R_{\odot}$. A color version is available online.

5. Conclusions

Within the present study we have shown that the hemispheric pattern of filaments, including exceptions, may be explained through the combined effects of differential rotation, meridional flow and surface diffusion, where these effect act on new magnetic bipoles, which emerge in each hemisphere containing the dominant sign of helicity for that hemisphere. Full solar cycle simulations show that the correct chirality may be found along the polar crown PIL as long as the simulations are run for long enough to remove the initial condition. Predictions for the hemispheric pattern have been made for the declining phase of the cycle which may now be tested with observations in Solar Cycle 24.

References

- Mackay, D. H. & van Ballegooijen, A. A. 2006, *ApJ*, 641, 577
 Martin, S. F., Bilimoria, R., & Tracadas, P. W. 1994, *Solar Surface Magnetism*, 303
 van Ballegooijen, A. A., Priest, E. R., & Mackay, D. H. 2000, *ApJ*, 539, 983
 Yang, W. H., Sturrock, P. A., & Antiochos, S. K. 1986, *ApJ*, 309, 383
 Yeates, A. R., Mackay, D. H., & van Ballegooijen, A. A. 2007, *Solar Phys.*, 245, 87
 Yeates, A. R., Mackay, D. H., & van Ballegooijen, A. A. 2008, *Solar Phys.*, 247, 103
 Yeates, A. R. & Mackay, D. H. 2009, *Solar Phys.*, 254, 77
 Yeates, A. R. & Mackay, D. H. 2012, *ApJL*, 753, L34
 Zirker, J. B., Leroy, J.-L., & Gaizauskas, V. 1997, *Solar Phys.*, 176, 279